PHYSICAL REVIEW B **79**, 180506(R) (2009)

Stabilization of hydrogen atoms in aggregates of krypton nanoclusters immersed in superfluid helium

R. E. Boltnev,[1,2] E. P. Bernard,[1] J. Järvinen,[1] V. V. Khmelenko,[1] and D. M. Lee[1]
[1]*Laboratory of Atomic and Solid State Physics, Cornell University, Ithaca, New York 14853, USA*
[2]*Branch of Institute of Energy Problems of Chemical Physics, Russian Academy of Sciences, Chernogolovka, Moscow Region 142432, Russia*
(Received 2 April 2009; published 14 May 2009)

Impurity-helium condensates (IHCs) containing krypton and hydrogen atoms immersed in superfluid ^{4}He have been studied via cw electron-spin-resonance (ESR) techniques. The IHCs are gel-like aggregates of nanoclusters composed of krypton and hydrogen atoms. We have found that very high average ($\sim 10^{19}$ cm^{-3}) and local ($\sim 6\times 10^{19}$ cm^{-3}) concentrations of hydrogen atoms can be stabilized in these samples. The analysis of ESR line positions and shapes shows that most of the H atom population resides in solid H_2 layers on the krypton nanocluster surfaces. High concentrations of atomic hydrogen achieved in IHCs provide an important step in the search for collective magnetic and quantum statistical phenomena at lower temperatures.

DOI: 10.1103/PhysRevB.79.180506 PACS number(s): 67.80.fh, 67.80.dk, 76.30.Rn, 61.46.−w

The study of H atoms trapped in solid H_2 is a fascinating area of research. An interesting feature of this system is that H atoms can move through solid H_2 via a tunneling process involving the exchange reaction $H+H_2 \rightarrow H_2+H$.[1] This phenomenon is evidence of quantum delocalization of the atoms. However, the same mechanism leads to the recombination of H atoms at $T \geq 1$ K.[2–6] Recently, it has been shown that at $T \leq 150$ mK the process of recombination is significantly suppressed as temperature is lowered due to the increased role of energy mismatch as two H atoms approach each other in solid H_2.[7] This may allow an approach of H atoms sufficiently close to manifest collective magnetic or quantum phenomena. Stable H atom concentrations of 10^{18} cm^{-3} were achieved in these experiments. For the observation of collective quantum phenomena, the thermal de Broglie wavelength must be larger than the distance between the H atoms. High concentrations of H atoms and low temperatures are required for this criterion to be met.

The main goal of this research program is to stabilize and cool high concentrations of H atoms so that collective phenomena resulting from their interactions can be studied. In this Rapid Communication we discuss studies of H atoms trapped in Kr nanoclusters in superfluid helium, which form a tenuous gel-like substance similar in structure to light aerogel. The strands of the sample consist of aggregates of impurity clusters, each 5–10 nm in diameter and surrounded by a monolayer of solid helium.[8–10] These samples are called impurity-helium solids or impurity-helium condensates (IHCs). We present cw (electron-spin-resonance) ESR measurements on atomic hydrogen free radicals in IHCs prepared from gas mixtures containing helium, krypton, and hydrogen. We found that addition of Kr atoms to the hydrogen-helium gas mixture dramatically increased the efficiency of stabilization of H atoms. Average concentrations of H atoms as high as $\sim 10^{19}$ cm^{-3} were attained in H-Kr IHCs. ESR line positions indicate that most of the stabilized H atoms reside in solid H_2 layers at the surfaces of the krypton nanoclusters immersed in superfluid helium.

The data were obtained with an apparatus and procedures closely resembling the cw ESR techniques used in earlier experiments.[11,12] A jet consisting of a mixture of helium and impurity gases was directed through the surface of superfluid helium contained in a collection beaker. Immediately prior to this, the gas passed through an electrical discharge that dissociated the molecules. The liquid level in the beaker ($T=1.5$ K) was maintained by a fountain pump placed in the main liquid helium bath in the lower portion of the cryostat. Following preparation, the samples were lowered into a TE_{011} *X* band cylindrical resonant cavity ($f_r=9.07$ GHz) located in the main liquid helium bath. Coils were installed outside the resonant cavity to modulate the applied field at a frequency of 100 kHz. This allowed lock-in detection of the derivative of the microwave absorption signal while the main applied field was slowly swept through an ESR line. This magnetic field H_0 was measured by an NMR magnetometer and the microwave frequencies were monitored by a frequency counter. Samples measured immediately following preparation and cooling are designated "as-prepared" samples. In a typical experimental run a series of ESR spectra were recorded at 1.35 K. In Figs. 1(a) and 1(b), we display spectra of H atoms contained in IHC samples prepared from gas mixtures with ratios H_2:Kr:He=1:1:200 and H_2:Kr:He=1:50:10 000, respectively. The high-field lines (HFLs) and the low-field lines (LFLs) of atomic hydrogen were separated by approximately 508 G. The LFLs exhibit a pronounced small feature on the high-field wing. A corresponding feature is not observed for the HFLs. The positions of the small features on both spectra as well as the positions of the HFLs coincide. On the contrary, the positions of the main LFLs are shifted by ~0.8 G relative to one another [Figs. 1(a) and 1(b)]. After observations were made at $T=1.35$ K, the samples were gradually heated to 14.5 K and then the samples were cooled again to 1.35 K. During annealing, recombination of H atoms into H_2 molecules greatly reduced the H atom concentration. This can be seen in Fig. 1(c), which corresponds to the sample shown in Fig. 1(a) after annealing. In addition, the LFL after annealing occurs almost exactly at the position of the small feature on the LFL

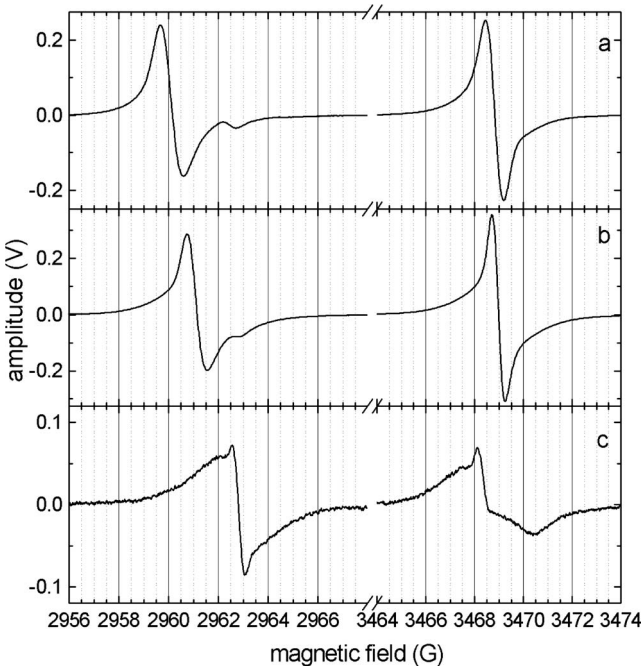

FIG. 1. [(a) and (b)] ESR spectra of hydrogen atoms in as-prepared H-Kr-He samples at 1.35 K. Samples were prepared from gas mixtures with the ratios H_2:Kr:He=1:1:200 and H_2:Kr:He=1:50:10 000, respectively. (c) ESR spectra of the sample shown in Fig. 1(a) after annealing to 14.5 K and cooling to 1.35 K. All spectra were obtained at 1.35 K. The amplification for measuring spectra of the annealed sample was increased by 15 times.

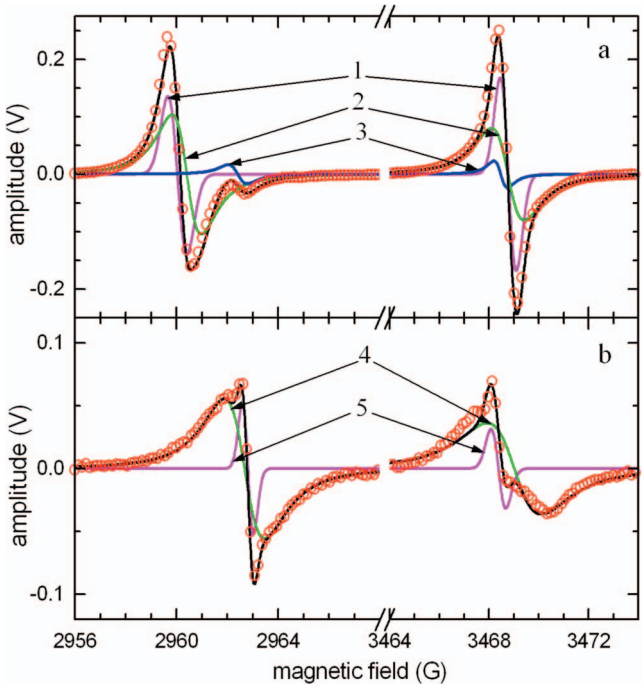

FIG. 2. (Color) (a) Experimental ESR spectra of H atoms for as-prepared H-Kr-He sample (open red circles) shown in Fig. 1(a) and three pairs of fitting lines [(1) magenta are Gaussian lines and (2) green and (3) blue are Lorentzian lines]. b) Experimental ESR spectra of H atoms for annealed sample (open red circles) shown in Fig. 1(c) and two pairs of fitting lines [(4) green are Lorentzian lines and (5) magenta are Gaussian lines]. The sums of fitting lines are shown as black lines for both a and b.

before annealing. After annealing, both the LFL and the HFL appear to consist of superpositions of a narrow line and a broad line as shown in Fig. 1(c). Spectra similar to those shown in Fig. 1(c) were obtained by the fast deposition of H and Kr atoms on cold substrates to form samples of H atoms embedded in disordered Kr lattices.[13]

The low- and high-field spectra displayed in Figs. 1(a) and 1(b) for the as-prepared samples were each fitted with a sum of one Gaussian and two Lorentzian lines as shown in Fig. 2(a) only for the sample corresponding to Fig. 1(a). Although Fig. 1(a) shows only two well-resolved peaks for the low-field line before annealing, three curves were required to adequately fit the data. The centers of the fitting curves were appreciably displaced from one another only for the case of the LFL. For the annealed sample the sum of two curves, one Lorentzian and one Gaussian, [Fig. 2(b)] were fitted to the data. The amplitudes and widths of the fitting curves were used to determine the number of unpaired spins corresponding to each curve by comparison with signals obtained from a ruby crystal with a known number of spins contained in the resonant cavity. The average concentrations were calculated by adding the number of spins for the LFL and HFL and dividing the result by the volume occupied by the sample. Dipolar magnetic coupling among the electron spins is the dominant line broadening mechanism in this system. This allows the concentration of the atomic radicals to be estimated by the following formula: $n_l = 2.7 \times 10^{19} \times \Delta H_{dd}$, where ΔH_{dd} is the peak to peak width of the ESR lines in Gauss and n_l is the local concentration of atoms per cm^3.[14] The positions of the fitting curves were used to calculate the g factors and the hyperfine constants A for H atoms in H-Kr-He samples by inverting the Breit-Rabi equation.[15] Table I lists the values of the hyperfine constants A in MHz and the g factors for the five pairs of fitting curves shown in Fig. 2. Curves 1–3 correspond to the as-prepared samples,

TABLE I. Hyperfine structure constants, A, and g factors for H atoms in H-Kr-He condensates, in H_2, and in Kr matrices.

Matrix	A, MHz	$\Delta A/A$, %	g factor
H-Kr-He, curve 1	1416.33(20)	−0.29	2.00228(5)
H-Kr-He, curve 2	1415.49(62)	−0.35	2.00220(16)
H-Kr-He, curve 3	1408.74(43)	−0.82	2.00176(11)
H-Kr-He, curve 4	1409.60(20)	−0.76	2.00160(5)
H-Kr-He, curve 5	1407.88(43)	−0.88	2.00178(11)
H-Kr-He, curve 1′	1414.71	−0.40	2.00199
H-Kr-He, curve 2′	1414.105	−0.45	2.00192
H-Kr-He, curve 3′	1409.935	−0.74	2.00158
Free state[19,20]	1420.40573(5)	0	2.002256(24)
H_2 [21]	1417.13(45)	−0.23	2.00243(8)
Kr (subst.)[16]	1411.799(30)	−0.61	2.00179(8)
Kr (subst.)[17]	1409	−0.80	2.0013
Kr (interst.)[16]	1427.06(280)	+0.47	1.99967(31)

and curves 4–5 represent the annealed samples. The data from analysis of Fig. 1(b) are represented in Table I by curves $1'-3'$.

Earlier investigations found that H atoms can occupy substitutional and interstitial sites in Kr matrices.[13,16,17] Deposition of H atoms and Kr atoms from the gas phase onto a cold substrate always results in the positioning of H atoms in substitutional sites of a Kr matrix.[13,16] Samples of H atoms embedded in solid Kr prepared by photolysis was studied by Foner *et al.*[16] and Vaskonen *et al.*[17] Both groups observed signals associated with substitutional and interstitial sites. Foner *et al.*[16] observed that their samples contained H atoms primarily in substitutional sites at 4.2 K. In the experiments of Vaskonen *et al.*[17] at higher temperatures, H atoms first occupied interstitial (octahedral) sites, but upon annealing at 24 K the H atoms migrated to substitutional sites. The values of g and A for substitutional and interstitial sites are listed in the lowest three entries of Table I. Adrian[18] gave a theoretical discussion of H atoms in solid inert gas lattices. His results gave reasonable quantitative agreement with the experimental values of g and A found for substitutional and interstitial sites of H atoms in a solid Kr matrix. Two other entries in Table I correspond to the g and A values obtained by other authors for free H atoms[19,20] and for H atoms trapped in solid H_2.[21]

The additional lines corresponding to curves 1 and 2 in Fig. 2(a) and corresponding entries in Table I have been observed for H-Kr systems in this work. It is clear that the values of g and A corresponding to curves 1 and 2 are in reasonable agreement with the values of g and A for H atoms embedded in solid H_2. This means that we have H atoms in thick layers of solid H_2 adsorbed on the surfaces of the Kr nanoclusters. In contrast, as shown in Table I, the values of g and A for curves $1'$ and $2'$ have shifted, indicating the influence of the Kr substrate. Therefore, we conclude that in the sample represented by Fig. 1(b), H atoms are embedded in a very thin H_2 film on Kr nanoclusters and are thus very close to the Kr substrate. On the other hand, the values of g and A for curves 3–5 in Table I correspond to H atoms embedded in substitutional sites in solid Kr.

We suggest the following explanation for the observed features of the ESR spectra of H atoms in H-Kr IHCs and their behavior during the annealing process: before annealing, we identify the large broad ESR signals in Figs. 1(a) and 1(b) as being associated with H atoms trapped in layers of solid H_2 at the surfaces of the Kr clusters comprising the IHCs. This fact is consistent with a model which predicts that a large fraction of the atomic-free radicals will lie on the cluster surfaces.[22] This occurs because the strong van der Waals forces between the Kr atoms lead to the formation of nanoclusters of nearly pure Kr at higher temperatures in the early stage of sample formation.[23] Then the more weakly attracted H atoms, H_2 molecules, and He atoms bind to the Kr cluster surfaces. The observed shift of the large LFLs seen in Figs. 1(a) and 1(b) and discussed above corresponds to different environments for H atoms for these two samples, depending on the thickness of the solid H_2 films adsorbed on the surfaces of Kr nanoclusters. Evidence for preferentially populating hydrogen or deuterium atoms on solid HD or D_2 cluster surfaces has previously been observed in pulsed ESR experiments.[24] In Fig. 2(a), curves 1 and 2 may correspond to H atoms at different sites in the films. The very small line [shoulder in Figs. 1(a) and 1(b) and line 3 in Fig. 2(a)] corresponds to H atoms trapped inside the Kr clusters. Upon annealing, the surface atoms diffuse rapidly and the clusters agglomerate into larger crystallites, destroying most of the surface population of the H atoms by recombination and leaving only a small population of H atoms trapped in the Kr matrices.

The average concentration of H atomic-free radicals in the sample prepared from a gas mixture with the ratio $H_2:Kr:He=1:1:200$ was 1.4×10^{18} cm^{-3} [see Fig. 1(a)]. The local concentration calculated from the dipolar broadening ($\Delta H=2.2$ G) was found to be 6×10^{19} cm^{-3}. The much larger local concentration is an expected consequence of the high porosity of the sample. We observed decay of the H atoms in the thick H_2 film in this sample during storage at $T=1.35$ K. The results showed a linear dependence of the reciprocal concentration of H atoms on time, indicating a second-order recombination process for the H atoms. To obtain the recombination rate constant $K_H(T)$, we used the equation $K_H(T)=(2n_0\tau_{1/2})^{-1}$, where n_0 is the initial concentration of H atoms and $\tau_{1/2}$ is the time needed to halve the initial concentration. With an initial concentration $n_0=1.4\times10^{18}$, we found a value of $\tau_{1/2}=161$ min, leading to a rate constant $K_H(1.35)=3.7\times10^{-23}$ cm^3/s. The recombination process is expected to be dominated by tunneling of the H atoms through the H_2 films on the Kr substrate. For thick H_2 films, the decay behavior of H atoms is similar to that found in the previous work on H in solid H_2, indicating that the reaction $H+H_2\rightarrow H_2+H$ provides a delocalization mechanism for H atoms.[1] Therefore, the H atoms in thick films on Kr cluster surfaces may be considered as indistinguishable, and we thus expect quantum statistical correlations for those atoms at very low temperatures. The analysis of fitting curves shown in Fig. 2(a) implies that 95% of the H atoms resided on the cluster surfaces and 5% of the H atoms were in the interior of the clusters. After annealing, only 5% of the initial population of atomic-free radicals survived and all of these surviving atoms were embedded in the Kr clusters. The decomposition of the ESR signal after annealing into a broad and narrow line [see Fig. 2(b)] may be attributed to segregation, driven by irregularities in the annealing process, into H atom rich regions with large dipolar interactions and H atom poor regions. An alternative explanation for similarly shaped spectra[13] is that the narrow lines correspond to substitutional fcc and hcp sites and the broad lines are from H atoms in disordered regions in the Kr lattice.

We have also studied seven other H-Kr-He samples by using gas mixtures with different ratios of $H_2:Kr$ from 1:5 to 1:50, reinforcing our conclusions. The largest concentration of 3.2×10^{18} cm^{-3} was obtained for the sample prepared from a gas mixture with ratio $H_2:Kr:He=1:50:10\,000$ [see Fig. 1(b)]. For this sample 97% of the atomic H-free radicals resided on the Kr cluster surfaces and 3% were embedded in the cluster interiors. After compression of this sample, the average concentration increased to 1.2×10^{19} cm^{-3}. For a typical Kr cluster size of 5 nm, the spacing between H atoms on the surface is ~1.4 nm. Remarkably, H atoms in these samples were stable during storage at $T=1.35$ K. The ab-

sence of recombination of H atoms in thin layers of H_2 does not necessarily mean the absence of their diffusion. Although the H atoms in very thin H_2 layers on Kr surfaces are expected to be more strongly influenced by the Kr substrate, leading to lower mobility of H atoms and smaller recombination rates at $T \sim 1.35$ K, the mobility of H atoms via tunneling reactions is not suppressed completely. This was evident in an experiment with the gas mixture HD:Kr:He=1:5:1200, where we observed a decrease in the D atom concentration with time and an equivalent increase in the H atom concentration. This is a consequence of the tunneling exchange reaction $D+HD \rightarrow D_2+H$, occurring on the Kr surface. The sum of concentrations of H and D atoms was constant in this experiment, also showing the absence of recombination in this sample. We find that the efficiency of stabilization of H atoms changes drastically for different gas mixtures. For example, for a gas mixture with a ratio H_2:Kr:He=1:1:200, the efficiency of H atom capture is only 0.5%, whereas for a gas mixture with a ratio H_2:Kr:He=1:50:10 000, the efficiency of H atom capture is 64%. The high capture rate and *absence* of recombination of H atoms for this latter sample indicates that a large fraction of the hydrogen atoms in the layer covering Kr nanoclusters surfaces are atomic-free radicals rather than partners in H_2 molecules. Some of the remaining sites on the Kr clusters surfaces are occupied by He atoms.

We conclude that a large preponderance of the atomic H free radicals are confined to the H_2 films on Kr cluster surfaces for our as-prepared samples. During the annealing process, the surface population disappears, leaving only the H atoms embedded in the Kr clusters, which are protected from recombination due to the slow diffusion of H through the dense solid Kr at low temperatures. We demonstrated that by changing the content of H atoms and H_2 molecules in the condensed Kr-He gas mixture, we can alter the thickness of the H-H_2 film formed on the surface of the Kr nanoclusters. Therefore, we can regulate the interaction between H atoms and the surface substrate to create the most favorable condition for stabilization of high concentrations of H atoms. These experiments have achieved the highest average and local concentrations of H atoms obtained so far in matrix isolation studies. The existence of a layer of helium and H_2 molecules covering the cluster surface provides an arena for the study of the diffusion and tunneling of H atoms. In this environment, samples containing high concentrations of H atoms may exhibit interesting magnetic properties and possible Bose-Einstein correlations associated with quantum overlap at lower temperatures.[7]

We thank NSF (Grant No. DMR 0504683) and CRDF (Grant No. RUP1-2841-CG-06) for supporting this research program. J.J. thanks the Academy of Finland (Grant No. 124998) and the Finnish Cultural Foundation.

[1] T. Miyazaki, *Atom Tunneling Phenomena in Physics, Chemistry, and Biology* (Springer, Berlin, 2004).
[2] S. I. Kiselev, V. V. Khmelenko, and D. M. Lee, Phys. Rev. Lett. **89**, 175301 (2002).
[3] E. B. Gordon, A. A. Pelmenev, O. F. Pugachev, and V. V. Khmelenko, JETP Lett. **37**, 282 (1983).
[4] A. V. Ivliev, A. Ya. Katunin, I. I. Lukashevich, V. V. Sklyarevskii, V. V. Suraev, V. V. Filippov, N. I. Filippov, and V. A. Shevtsov, JETP Lett. **36**, 472 (1982).
[5] H. Tsuruta, T. Miyazaki, K. Fueki, and N. Azuma, J. Phys. Chem. **87**, 5422 (1983).
[6] T. Miyazaki, K.-P. Lee, K. Fueki, and A. Takeuchi, J. Phys. Chem. **88**, 4959 (1984).
[7] J. Ahokas, J. Järvinen, V. V. Khmelenko, D. M. Lee, and S. Vasiliev, Phys. Rev. Lett. **97**, 095301 (2006).
[8] E. B. Gordon, V. V. Khmelenko, A. A. Pelmenev, E. A. Popov, and O. F. Pugachev, Chem. Phys. Lett. **155**, 301 (1989).
[9] V. Kiryukhin, B. Keimer, R. E. Boltnev, V. V. Khmelenko, and E. B. Gordon, Phys. Rev. Lett. **79**, 1774 (1997).
[10] S. I. Kiselev, V. V. Khmelenko, D. M. Lee, V. Kiryukhin, R. E. Boltnev, E. B. Gordon, and B. Keimer, Phys. Rev. B **65**, 024517 (2001).
[11] E. B. Gordon, A. A. Pelmenev, and O. F. Pugachev, and V. V. Khmelenko, Sov. J. Low Temp. Phys. **8**, 299 (1982).
[12] S. I. Kiselev, V. V. Khmelenko, E. P. Bernard, and D. M. Lee, Low Temp. Phys. **29**, 505 (2003).
[13] Yu. A. Dmitriev, Low Temp. Phys. **33**, 493 (2007).
[14] C. Kittel and E. Abrahams, Phys. Rev. **90**, 238 (1953).
[15] G. Breit and I. I. Rabi, Phys. Rev. **38**, 2082 (1931).
[16] S. N. Foner, E. L. Cochran, V. A. Bower, and C. K. Jen, J. Chem. Phys. **32**, 963 (1960).
[17] K. Vaskonen, J. Eloranta, T. Kiljunen, and H. Kunttu, J. Chem. Phys. **110**, 2122 (1999).
[18] F. J. Adrian, J. Chem. Phys. **32**, 972 (1960).
[19] P. Kusch, Phys. Rev. **100**, 1188 (1955).
[20] R. Beringer and M. A. Heald, Phys. Rev. **95**, 1474 (1954).
[21] C. K. Jen, S. N. Foner, E. L. Cochran, and V. A. Bower, Phys. Rev. **104**, 846 (1956).
[22] E. B. Gordon, Low Temp. Phys. **30**, 756 (2004).
[23] V. Kiryukhin, E. P. Bernard, V. V. Khmelenko, R. E. Boltnev, N. V. Krainyukova, and D. M. Lee, Phys. Rev. Lett. **98**, 195506 (2007).
[24] E. P. Bernard, V. V. Khmelenko, and D. M. Lee, J. Low Temp. Phys. **150**, 516 (2008).